

Inhibition of SHP2 and SHP1 Protein Tyrosine Phosphatase Activity by Chemically Induced Dimerization

Sara J. S. Buck, Bailey A. Plaman, and Anthony C. Bishop*

Cite This: *ACS Omega* 2022, 7, 14180–14188

Read Online

ACCESS |



Metrics & More

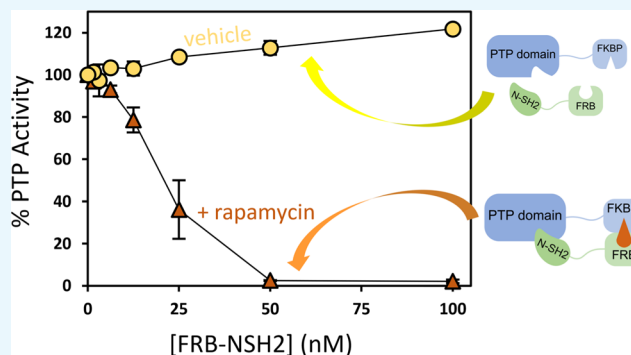


Article Recommendations



Supporting Information

ABSTRACT: Protein tyrosine phosphatases (PTPs), the enzymes that catalyze the dephosphorylation of phosphotyrosine residues, are important regulators of mammalian cell signaling, whose activity is misregulated in numerous human diseases. PTPs are also notoriously difficult to selectively modulate with small molecules, and relatively few small-molecule tools for controlling their activities in the context of complex signaling pathways have been developed. Here, we show that a chemical inducer of dimerization (CID) can be used to selectively and potently inhibit constructs of Src-homology-2-containing PTP 2 (SHP2) that have been engineered to contain dimerization domains. Our strategy was inspired by the naturally occurring mechanism of SHP2 regulation, in which the PTP activity of SHP2's catalytic domain is autoinhibited through an intramolecular interaction with the protein's N-terminal SH2 (N-SH2) domain. We have re-engineered this inhibitory interaction to function intermolecularly by independently fusing the SHP2 catalytic and N-SH2 domains to protein domains that heterodimerize upon the introduction of the CID rapamycin. We show that rapamycin-induced protein dimerization leads to potent inhibition of SHP2's catalytic activity, which is driven by increased proximity of the SHP2 catalytic and N-SH2 domains. We also demonstrate that CID-based inhibition of PTP activity can be applied to an oncogenic gain-of-function SHP2 mutant (E76K SHP2) and to the catalytic domain of the SHP2's closest homologue, SHP1. In sum, CID-driven inhibition of PTP activity provides a broadly applicable tool for inhibiting dimerizable forms of the SHP PTPs and represents a novel paradigm for selective PTP inhibition through inducible protein–protein interactions.



INTRODUCTION

Protein tyrosine phosphatases (PTPs) are enzymes that catalyze the hydrolytic removal of phosphate groups from phosphorylated tyrosine residues in mammalian signal-transduction pathways.¹ Aberrant PTP activity has been implicated in a wide variety of pathologies,^{2–6} but the precise connections between PTP dysregulation and human disease are often unclear. Small-molecule tools that can specifically control the activity of PTPs would represent valuable tools for studying the signaling pathways in which PTPs are involved and elucidating the molecular connections between misregulated PTPs and their associated pathologies.

Unfortunately, relatively few validated chemical tools for controlling PTP activity in a cellular context are known. Despite some notable exceptions, active-site-directed PTP inhibitors generally possess limited selectivity and cellular permeability.^{7–9} Allosteric approaches potentially hold more promise for target-specific PTP engagement, and selective allosteric inhibitors have been developed for a few PTPs.^{10–16} However, targetable allosteric sites have not been identified on the majority of human PTPs, and systematic means for uncovering PTP allosteric sites have not been described. Moreover, even well-characterized allosteric inhibitors can be

rendered ineffective by disease-associated mutations in a target PTP.^{17–19} Therefore, the development of complementary means of modulating PTP activity is important to enable the study of the pathways in which PTPs are involved. Previous work in our lab has led to the development of chemical tools that selectively modulate the activity of rationally engineered (“sensitized”) PTPs,^{20–23} but these approaches have had limited success in application to cellular systems due to compound bioavailability issues similar to those that hamper active-site-directed strategies. In the current study, we investigate whether protein engineering can be used to sensitize PTPs to selective inhibition using a system that has previously been validated for controlling protein function in cells—namely, the use of chemical inducers of dimerization (CIDs).^{24–26}

Received: February 7, 2022

Accepted: March 21, 2022

Published: April 11, 2022



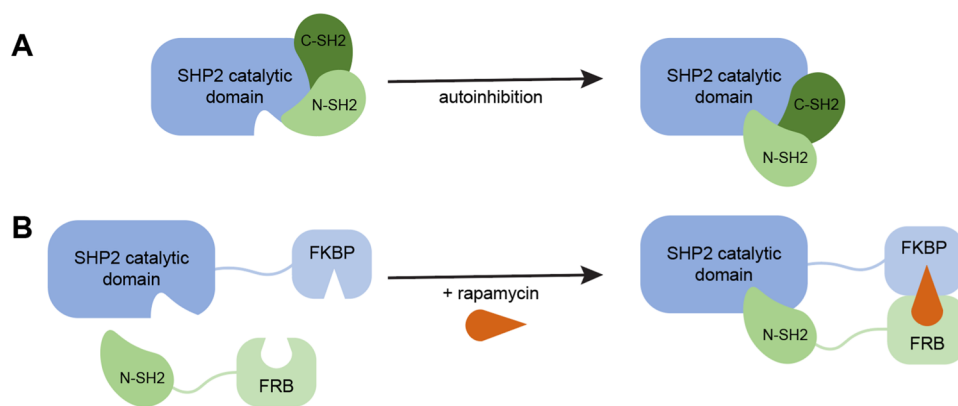


Figure 1. Design of chemically dimerizable SHP2. (A) Schematic of autoinhibition in wild-type SHP2. The CD (blue) is inhibited by the SH2 domains (green). (B) Schematic of inhibition in a chemically dimerizable SHP2 CD/N-SH2 system. The SHP2 CD is fused to FKBP (blue) and N-SH2 is fused to FRB (green). FKBP dimerizes with FRB upon addition of rapamycin, bringing SHP2 CD and N-SH2 into close proximity to induce inhibition of SHP2 CD's PTP activity.

CIDs are broadly useful tools that can control protein–protein interactions in a cellular context. One of the most widely applied CIDs, the natural product rapamycin, forms a high-affinity ternary complex with the FK506-binding protein (FKBP) and the FKBP-rapamycin-binding (FRB) domain of the mammalian target of rapamycin kinase.²⁷ FKBP and FRB, both small in size, can be fused to proteins of interest (POIs) via flexible linkers such that, upon addition of rapamycin, the POIs are brought into close proximity. Cellular applications of rapamycin and other CIDs are numerous and wide-ranging.^{24–26} To provide just one specific example, rapamycin has previously been used to chemically rescue the activity of “split” PTPs—half PTP domains that demonstrate phosphatase activity only when they are brought into close proximity with their complementary halves by the CID.²⁸ Could a CID be used in the functionally opposite fashion to specifically induce PTP inhibition upon dimerization? If a low-affinity inhibitory protein for a target PTP could be identified, it may be hypothesized that inducing dimerization between the PTP and the inhibitor would dramatically increase the latter's local concentration and, as a result, its inhibitory potency. A CID could therefore be a useful chemical tool to selectively induce inhibition of a target PTP, if a suitable low-affinity inhibitory protein can be identified.

In the current study, we investigate the use of a protein domain from Src-homology-2-containing PTP 2 (SHP2) as a dimerizable inhibitor of PTP activity. SHP2 is a ubiquitously expressed and widely studied PTP that has been implicated in a variety of diseases.^{29,30} The SHP2 protein comprises a catalytic PTP domain and two Src-homology-2 (SH2) domains, and, in its basal state, SHP2 adopts an autoinhibited conformation in which the N-terminal SH2 (N-SH2) domain intramolecularly obstructs the catalytic site of the PTP domain.^{31,32} Upon activation by a phosphotyrosine-containing binding partner, N-SH2 shifts away from the catalytic site, and the enzyme becomes active.^{17,18,31,32} Previous work has shown that the isolated N-SH2 domain can function as a SHP2 inhibitor—that is, independently expressed N-SH2 inhibits the activity of the SHP2 catalytic domain (CD) intermolecularly but only with low potency.³³ In this study, we explore whether the potency of PTP inhibition by isolated N-SH2 can be improved by inducing an increase in its local concentration. To address this question, we turned to the aforementioned rapamycin-based CID system. We hypothesized that if FKBP

and FRB were fused to the SHP2 CD and N-SH2 domains, rapamycin treatment could bring the two domains into proximity, inducing potent and selective inhibition of SHP2 CD's PTP activity.

RESULTS AND DISCUSSION

Design and Validation of Dimerizable SHP2 Constructs. In the absence of a stimulus, wild-type SHP2 predominately exists in a conformation in which the CD is autoinhibited by its two SH2 domains.³¹ In this “closed” conformation, N-SH2 makes contact with residues surrounding the active site of the CD (Figure 1A).³² To potentially recreate this interaction in a CID-inducible system, we fused the dimerization domains FRB and FKBP to the isolated N-SH2 and CDs of SHP2, respectively. The domains were attached using a 15-amino-acid poly serine/glycine linker to generate FRB-NSH2 and FKBP-SHP2CD (Figures 1B and S1). In this system, the introduction of rapamycin should dimerize FRB and FKBP, potentially bringing N-SH2 into close proximity with the SHP2 CD to induce potent inhibition of the latter's PTP activity (Figure 1B).

To validate that the added linker and dimerization domain do not impede N-SH2's function, we assessed the inhibitory activities of isolated N-SH2 and FRB-NSH2 on SHP2 CD. Consistent with previous findings,³³ we first confirmed that N-SH2 is a very weak inhibitor of SHP2 CD; we measured its 50% inhibitory concentration (IC₅₀) to be approximately 15 μM (Figure S2). We then tested whether the fusion with FRB affected N-SH2's potency and found that the added domain had no measurable effect: when tested at equal concentrations, N-SH2 and FRB-NSH2 inhibited SHP2 CD's PTP activity equivalently in either the absence or presence of rapamycin (Figure 2A). It is also important to note that addition of rapamycin itself had no measurable effect on SHP2 CD's PTP activity, regardless of the presence (or not) of the N-SH2 constructs (Figure 2A).

We subsequently measured the kinetic parameters of SHP2 CD and FKBP-SHP2CD to ensure that the addition of the dimerizable domain and linker did not dramatically alter SHP2 CD's inherent PTP activity. We found that although FKBP-SHP2CD demonstrated a somewhat reduced activity as compared to SHP2 CD, the catalytic efficiencies (k_{cat}/K_M) of the two enzymes were comparable (Figure 2B).

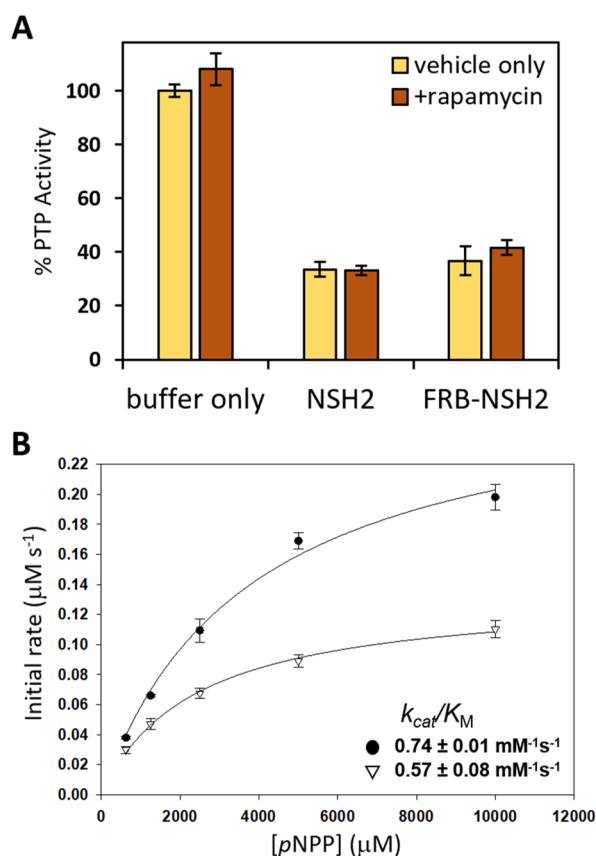


Figure 2. Effects of dimerization–domain fusion on N-SH2 and SHP2 CD. (A) The PTP activity of the SHP2 CD (25 nM) was assayed with 6,8-difluoro-4-methylumbelliferyl phosphate (DiFMUP) (100 μM) in the presence of N-SH2 (27.6 μM) or FRB-NSH2 (27.6 μM) in either the absence (yellow) or presence (orange) of 50 nM rapamycin. The dimethyl sulfoxide (DMSO) concentration was 1.5%. The data are normalized to the SHP2 CD activity with the buffer only in the absence of rapamycin. (B) Michaelis–Menten curves of the SHP2 CD and FKBP-SHP2CD. The SHP2 CD (100 nM, black circles) and FKBP-SHP2CD (100 nM, white triangles) were assayed for PTP activity with *para*-nitrophenyl phosphatase (*p*NPP) at the indicated concentrations.

Chemically Induced Inhibition of FKBP-SHP2CD by FRB-NSH2. We next sought to test whether dimerization can be used to increase the potency of PTP inhibition by N-SH2. To do so, we measured the PTP activity of FKBP-SHP2CD after treatment with varying concentrations of FRB-NSH2 in the absence or presence of rapamycin (Figure 3A). [It should be noted that the concentrations of the inhibitory protein FRB-NSH2 used in the dimerization experiment (Figure 3A, 0–100 nM) are orders of magnitude lower than the concentration used previously with the non-dimerizable SHP2 CD (Figure 2A, 27.6 μM) based on the hypothesis that dimerization could dramatically increase FRB-NSH2's inhibitory potency.] We found that FRB-NSH2 concentrations up to 100 nM had no significant effect on the FKBP-SHP2CD PTP activity in the absence of rapamycin. By contrast, strong, dose-dependent inhibition of FKBP-SHP2CD by FRB-NSH2 was observed in the presence of rapamycin. FRB-NSH2's rapamycin-dependent inhibitory effect was remarkably potent, with a 50% inhibitory concentration (IC₅₀) value of approximately 20 nM (Figure 3A). In fact, FRB-NSH2 potently inhibits FKBP-SHP2CD in the presence of rapamycin that its IC₅₀ value approaches the

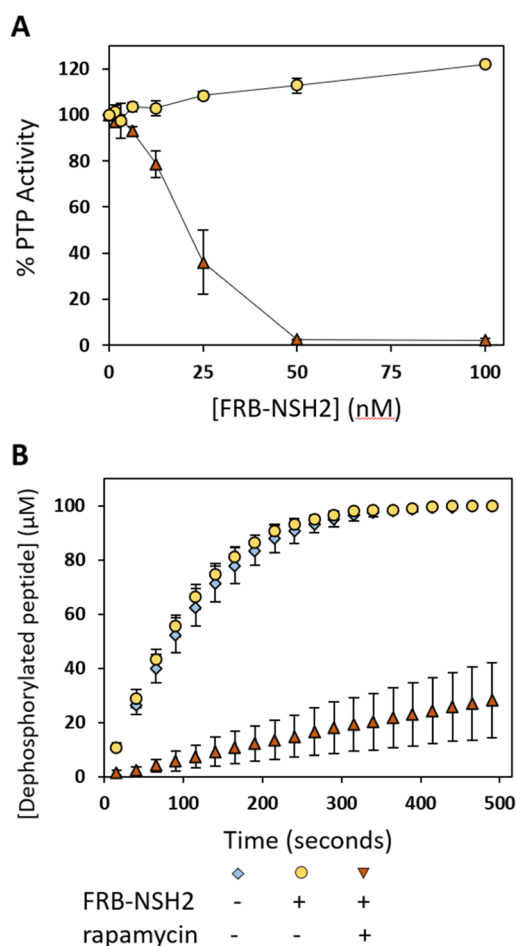


Figure 3. Rapamycin-dependent inhibition of FKBP-SHP2CD by FRB-NSH2. (A) Dose dependence of FKBP-SHP2CD inhibition. The PTP activity of FKBP-SHP2CD (25 nM) was measured with DiFMUP (100 μM) in the presence of the indicated concentrations of FRB-NSH2 in either the absence (yellow circles) or presence of 200 nM rapamycin (orange triangles). The DMSO concentration was 1.0%. (B) The activity of FKBP-SHP2CD (50 nM) was measured with the phosphopeptide DADEpYLIPQQG (100 μM) as a substrate after 15 min of pre-incubation in the absence (blue diamonds) or presence of FRB-NSH2 (50 nM) in either the absence (yellow circles) or presence (orange triangles) of rapamycin (100 nM). The DMSO concentration was 0.5%.

concentration of the enzyme in the assay (20 nM). Under the conditions of such a potent inhibition, the measured IC₅₀ value is limited by the enzyme concentration, and we therefore hypothesize that 20 nM IC₅₀ is actually a significant underestimation of FRB-NSH2's potency of inhibition. It is likely that the true inhibitory potency is governed by the extremely strong affinity of the FKBP-rapamycin-FRB ternary complex ($K_d \approx 100$ fM).³⁴ To further probe the mechanism of inhibition by FRB-NSH2, we tested the (ir)reversibility of its interaction with FKBP-SHP2CD. We found the inhibition to be irreversible as copious washing of dimerized FKBP-SHP2CD/FRB-NSH2 did not restore the PTP activity to FKBP-SHP2CD (Figure S3). These results are consistent with the previously characterized irreversibility of the FRB-rapamycin-FKB ternary complex formation.^{24–26}

The initial characterization of FKBP-SHP2CD and its inhibition by FRB-NSH2 were carried out with the small-molecule PTP substrates *p*NPP and DiFMUP. We next tested

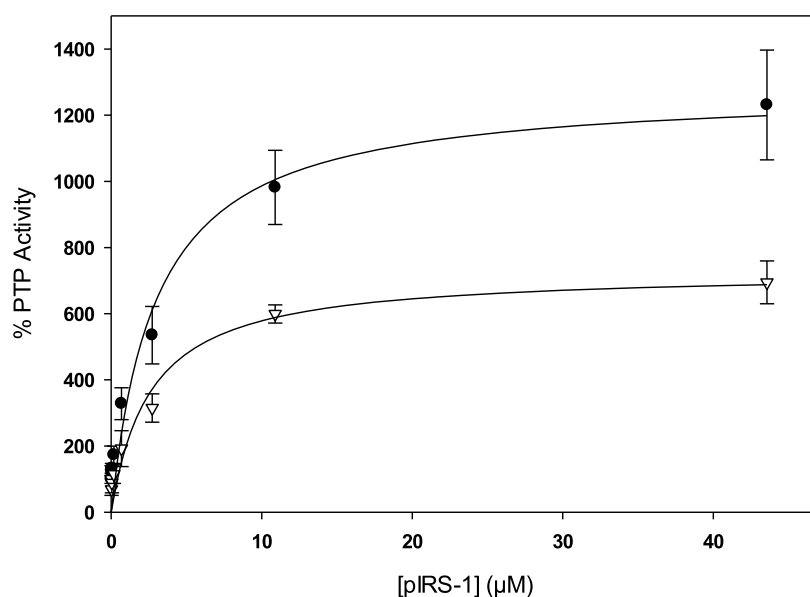


Figure 4. Activation of wild-type SHP2 and dimerized FKBP-SHP2CD/FRB-NSH2 with pIRS-1. The activities of wild-type SHP2 (50 nM, black circles) and dimerized FRB-NSH2/FKBP-SHP2CD (50 nM of each protein with 500 nM rapamycin, white triangles) were measured with DiFMUP (100 μ M) after a 15 min pre-incubation with the indicated concentrations of the phosphopeptide pIRS-1. The DMSO concentration was 2.0%.

whether FRB-NSH2 could effectively inhibit SHP2's dephosphorylation of more physiologically relevant substrates, such as phosphotyrosyl-containing peptides. This question was addressed using a phosphopeptide derived from an autophosphorylation site on the epidermal growth factor receptor (DADEpYLIPQQG).³⁵ Dephosphorylation of DADEpYLIPQQ by FKBP-SHP2CD was monitored in the presence of both rapamycin and FRB-NSH2, in the presence of only FRB-NSH2, and in the absence of both. Consistent with the previous findings on small-molecule substrates, FRB-NSH2 had no effect on the rate of DADEpYLIPQQ dephosphorylation in the absence of rapamycin, whereas the addition of rapamycin induced a strong inhibition of the PTP activity (Figure 3B). The ratio of the inhibitor (FRB-NSH2) to the enzyme (FKBP-SHP2CD) in the peptide-dephosphorylation assay was only 1:1, providing further evidence that the extremely high affinity of the CID-containing ternary complex can give rise to an excellent potency of PTP inhibition by FRB-NSH2.

Activation of FRB-NSH2/FKBP-SHP2CD with an SH2-Binding Phosphopeptide. As described previously, SHP2's cellular phosphatase activity is controlled by an intramolecular autoinhibitory interaction between its catalytic PTP domain and N-SH2; in SHP2's autoinhibited state, the N-SH2 domain blocks the PTP domain's active site.^{31,32,36} In cell-signaling pathways, SHP2 is activated when N-SH2's phosphotyrosine-binding pocket engages a phosphorylated protein target. The binding event transmits a conformational change and thereby disrupts the inter-domain inhibitory interaction and increases SHP2's PTP activity.^{31,32,36} SHP2's activation mechanism can be recreated in vitro with SH2-binding peptides; for example, a monophosphorylated peptide derived from insulin receptor substrate 1 (pIRS-1; SLNpYIDLVLK) has been previously shown to increase SHP2's PTP activity.¹⁷ Inspired by SHP2's cellular mechanism of autoinhibition and activation, we sought to test whether dimerized—and therefore inhibited—FRB-NSH2/FKBP-SHP2CD could be activated by the addition of

an SH2-binding peptide. As a positive control, we added increasing concentrations of pIRS-1 to SHP2 and observed that SHP2's PTP activity increased dramatically in a dose-dependent fashion, plateauing at approximately 12 times its basal level (Figure 4). We then investigated whether previously dimerized FKBP-SHP2CD/FRB-NSH2 could be similarly activated by pIRS-1. We found that the activity of dimerized FKBP-SHP2CD/FRB-NSH2 also increased strongly in the presence of pIRS-1. Activation of FKBP-SHP2CD/FRB-NSH2 exhibited a dose-response behavior similar to that of SHP2 as the concentration of pIRS-1 required to achieve half-maximal activation was approximately 3 μ M for both enzymes. However, the activity of pIRS-1-treated FKBP-SHP2CD/FRB-NSH2 plateaued at approximately 6 times its basal level, a lower value than was observed for SHP2 (Figure 4). These data suggest that the pIRS-1 affinities of FRP-NSH2 and N-SH2 within the context of full-length SHP2 are similar but that pIRS-1 treated FKBP-SHP2CD/FRB-NSH2 cannot adopt the fully active "open" SHP2 structure that has been characterized for SHP2.^{17,18} This observation may not be surprising given that FKBP-SHP2CD/FRB-NSH2 lacks SHP2's second SH2 domain (C-terminal SH2), which constitutes an integral part of the enzyme's open structure and is thought to facilitate the phosphopeptide binding that drives the activation of SHP2 in vivo.³¹

Chemically Induced Inhibition of an Oncogenic SHP2 Mutant. Hyperactivation of SHP2 has been widely associated with human cancers. In particular, gain-of-function (GOF) point mutations that disrupt the basal autoinhibition of SHP2 have been established as causative agents for leukemia.^{30,37–39} Small-molecule stabilizers of SHP2's autoinhibition (e.g., SHP099) hold enormous promise for targeting some cancers in which the SHP2 activity is implicated.¹⁰ However, the potency of SHP099 and the related compounds is strongly attenuated by cancer-associated GOF mutations that disrupt the integrity of the autoinhibitory interaction, and many of these molecules fail to inhibit highly activated SHP2 mutants

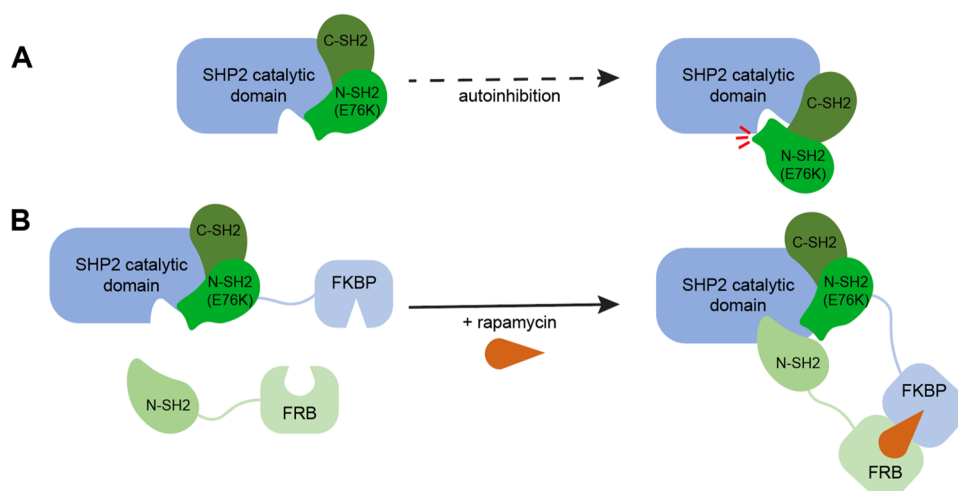


Figure 5. Design of chemically dimerizable E76K SHP2. (A) Schematic of autoinhibition in E76K SHP2. The E76K point-mutation in N-SH2 disrupts the autoinhibition of the CD (blue) by the SH2 domains (green). (B) Schematic of inhibition in a chemically dimerizable E76K SHP2/N-SH2 system. E76K SHP2 is fused to FKBP (blue) and the wild-type N-SH2 domain is fused to FRB. FKBP dimerizes to FRB upon addition of rapamycin, bringing E76K SHP2 and the functional N-SH2 domain into close proximity.

effectively.^{17–19} For example, the most highly activated leukemia-causing GOF SHP2 mutant, E76K SHP2, is only weakly inhibited by SHP099 due to a glutamate-to-lysine point mutation on N-SH2 that renders the domain ineffective for autoinhibition (Figure 5A).^{17,40} We hypothesized that our dimerization strategy could be used to bring a functional N-SH2 into close proximity with a GOF SHP2 mutant to afford chemically inducible inhibition of the mutant's PTP activity. Further, we surmised that the potency of CID-induced inhibition would be independent of the strength of the SH2/PTP domain interaction in the targeted GOF variant, and, therefore, the dimerization strategy may be effective for targeting even highly activated GOF mutants, such as E76K SHP2 (Figure 5B).

To test the idea that CIDs could be used to target GOF SHP2 mutants with high potency, we designed a dimerizable construct of E76K SHP2 that contains FKBP at its amino terminus (FKBP-(E76K)SHP2, Figures 5B and S4), and we confirmed using kinetic analysis that the addition of FKBP does not substantially affect E76K SHP2's inherent catalytic efficiency (Figure S5). Subsequently, we investigated the inhibition of FKBP-(E76K)SHP2-catalyzed DiFMUP dephosphorylation by FRB-N-SH2 in the absence and presence of rapamycin. We observed that FRB-N-SH2 gave rise to potent rapamycin-dependent inhibition (Figure 6A), akin to that observed previously with FKBP-SHP2CD (Figure 3A). FRB-N-SH2's IC_{50} in the presence of rapamycin (~ 45 nM) approaches the concentration of FKBP-(E76K)SHP2 in the assay (25 nM), again suggesting that the observed IC_{50} underestimates the potency of inhibition. Also, as observed previously with FKBP-SHP2 CD, FRB-N-SH2 had no effect on FKBP-(E76K)SHP2's activity in the absence of rapamycin (Figure 6A), demonstrating that potent inhibition of FKBP-(E76K)SHP2 by FRB-N-SH2 is driven by dimerization. Finally, we confirmed that rapamycin-inducible inhibition of FKBP-(E76K)SHP2 is not dependent on the choice of substrate in the assay as comparable results were obtained with the phosphopeptide substrate DADEpYLIPQQG (Figure 6B).

We next sought to compare the potencies of E76K SHP2 inhibition by dimerization and by the widely used allosteric SHP2 inhibitor, SHP099. As noted above, SHP099 works by

stabilizing SHP2's autoinhibited conformation, but the compound's potency is attenuated by GOF mutations.^{17–19} We confirmed that SHP099 only weakly inhibits FKBP-(E76K)SHP2 with an IC_{50} of approximately 10 μ M (Figure 6C), which is broadly consistent with previously reported IC_{50} values for SHP099 and E76K SHP2.^{17,19} We then analyzed the dose-dependence of rapamycin-induced inhibition of FKBP-(E76K)SHP2 in the presence of a fixed concentration of FRB-N-SH2 (Figure 6C). Consistent with the earlier experiment in which FRB-N-SH2 concentrations were varied (Figure 6B), we observed a very potent inhibition of FKBP-(E76K)SHP2 by rapamycin, with an IC_{50} (~ 10 nM) that is at the theoretical limit set by the 25 nM concentration of FKBP-(E76K)SHP2 in the assay (Figure 6C). These data establish that rapamycin-induced inhibition of FKBP-(E76K)SHP2 is at least 1000-fold more potent than its inhibition by SHP099, and it is likely that the difference is actually substantially greater as rapamycin's observable IC_{50} is limited by the assay conditions.

Chemically Induced Inhibition of SHP1 Activity. At a first glance, the CID-based approach for PTP inhibition described in this study appears to be applicable only to SHP2 and its GOF mutants as proximity is used to induce an inter-domain interaction that occurs naturally only in the SHP2 protein. Based on the structural conservation of PTP domains however, we surmised that a dimerizable SHP2 N-SH2 domain could potentially represent a more general tool for controlling the activities of dimerizable PTP domains, and we sought to investigate the idea that induced proximity between FRB-N-SH2 and a non-SHP2 PTP domain could also be used to effect PTP inhibition through a “non-natural” N-SH2/PTP interaction.

As a preliminary test of this hypothesis, we selected the CD of SHP2's closest homologue, SHP1 (SHP1 CD), which shares a 60% identity with SHP2 CD.⁴¹ Previous studies with SHP1/2 chimeric proteins have suggested that SHP2's SH2 domains can interact with SHP1's PTP domain,⁴² and we found that the isolated SHP2 N-SH2 domain is capable of inhibiting SHP1 CD's PTP activity in vitro, albeit weakly ($IC_{50} > 155$ μ M; Figure S6). To generate a dimerizable construct of SHP1 CD, we fused FKBP using a linker to SHP1 CD's amino terminus (FKBP-SHP1CD, Figure S7), and we confirmed using

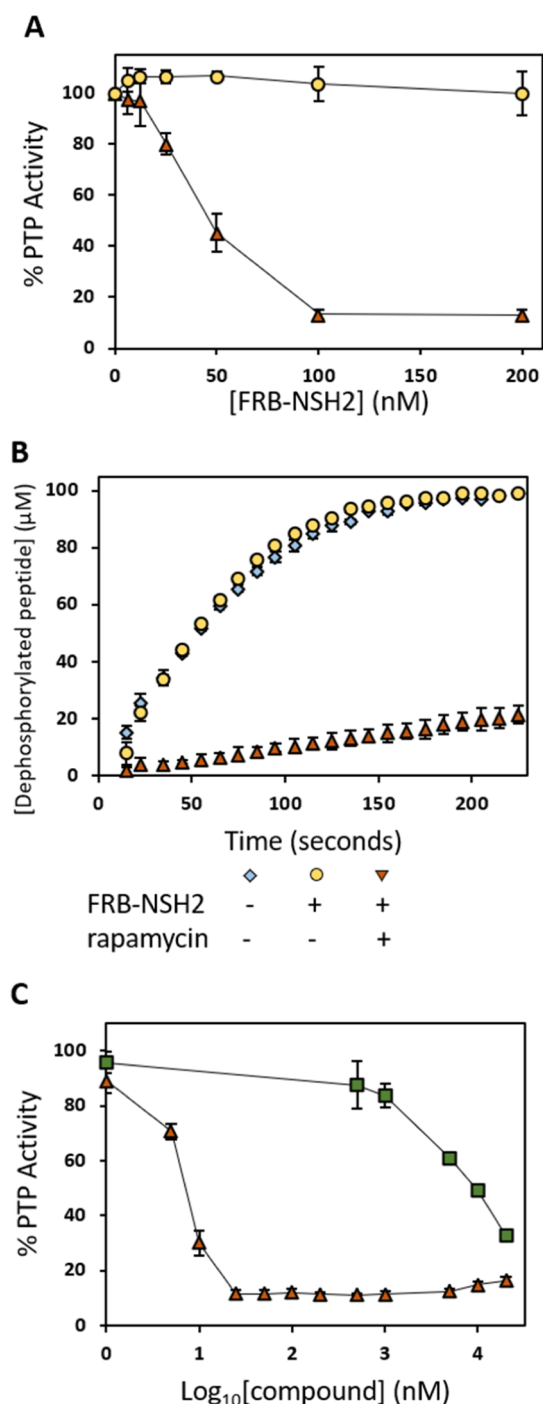


Figure 6. Rapamycin-dependent inhibition of FKBP-(E76K)SHP2 by FRB-NSH2. (A) The PTP activity of FKBP-(E76K)SHP2 (25 nM) was measured with DiFMUP (50 μ M) in the absence or presence of the indicated concentrations of FRB-NSH2 in either the absence (yellow circles) or presence of 500 nM rapamycin (orange triangles). The DMSO concentration was 1.0%. (B) The activity of FKBP-(E76K)SHP2 (50 nM) was measured with the phosphopeptide DADEpYLIPQQG (100 μ M) as a substrate after 15 min of pre-incubation in the absence (blue diamonds) or presence of FRB-NSH2 (250 nM) in either the absence (yellow circles) or presence (orange triangles) of 200 nM rapamycin. The DMSO concentration was 0.5%. (C) The PTP activity of FKBP-(E76K)SHP2 (25 nM) was measured with DiFMUP (50 μ M) in the presence of SHP099 (green squares) at the indicated concentrations or FRB-NSH2/rapamycin (orange triangles), with FRB-NSH2 at 100 nM and rapamycin at the indicated concentrations. The DMSO concentration was 5.0%.

Michaelis–Menten kinetic analysis that the addition of FKBP does not affect SHP1 CD's catalytic activity (Figure S8). We next investigated the ability of FRB-NSH2 to inhibit FKBP-SHP1CD's activity in both the absence and presence of rapamycin. We observed that FRB-NSH2 is a potent inhibitor of FKBP-SHP1CD ($IC_{50} \approx 90$ nM) under dimerizing conditions (Figure 7A). As observed in all instances of FRB-

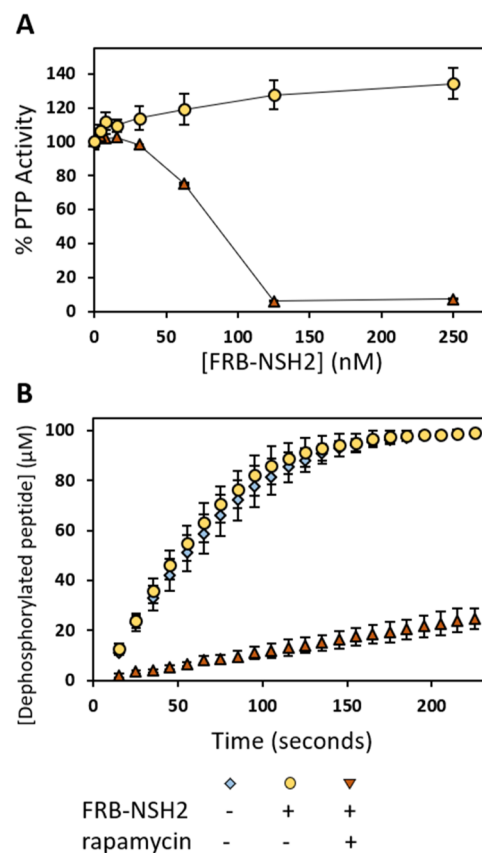


Figure 7. Rapamycin-dependent inhibition of FKBP-SHP1CD by FRB-NSH2. (A) The PTP activity of FKBP-SHP1CD (25 nM) was measured with DiFMUP (50 μ M) in the presence of the indicated concentrations of FRB-NSH2 in either the absence (yellow circles) or presence of 50 nM rapamycin (orange triangles). The DMSO concentration was 1.0%. (B) The activity of FKBP-SHP1CD (50 nM) was measured with the phosphopeptide DADEpYLIPQQG (100 μ M) as a substrate after 15 min of pre-incubation in the absence (blue squares) or presence of FRB-NSH2 (250 nM) in either the absence (yellow circles) or presence (orange triangles) of rapamycin (200 nM). The DMSO concentration was 0.5%.

NSH2-mediated inhibition in this study, FKBP-SHP1CD inhibition was found to be completely dependent on the presence of rapamycin (Figure 7A) and independent of the substrate used in the assay (Figure 7B). These data demonstrate that, even for an N-SH2/PTP-domain interaction that does not occur in nature, proximity can be a key driving force for N-SH2-mediated PTP inhibition.

CONCLUSIONS

Prospects for the Application of CID-Mediated Inhibition to Other PTPs. In the current study, we describe the design and application of a CID-based system that can be used to target dimerizable constructs of SHP2 and SHP1 for specific inhibition by SHP2's N-SH2 domain. In all the cases

investigated, CID-mediated SHP2/SHP1 inhibition is highly potent and independent of the PTP substrate used in the assay. Might an analogous system be used for PTPs beyond the SHP1/SHP2 subfamily? In a preliminary test of this hypothesis with an FKBP-linked PTP domain from outside the SHP1/SHP2 subfamily (PTP1B, 39% PTP domain identity with SHP2 CD), we have not observed dimerization-inducible inhibition with FRB-NSH2 (data not shown). We suspect, based on this finding, that FRB-NSH2 will only be useful for targeting dimerizable SHP2 and SHP1 constructs and that further protein engineering and/or discovery would be required to identify “weak” inhibitory domains whose affinity can be augmented through dimerization for PTPs outside the SHP1/SHP2 subfamily.

Prospects for Application of CID-Mediated Inhibition in Cellular Systems. Given the *in vitro* proof of concept provided in the current study and that CIDs have proven to be widely applicable in cellular systems, we believe that CID-induced inhibition of dimerizable SHP2 and SHP1 constructs will be functional for studies in mammalian cells. We further hypothesize that proximity-induced SHP2 or SHP1 inhibition by N-SH2 would work with CIDs other than rapamycin (e.g., “rapalogs” or abscisic-acid-based CIDs) if researchers wish to induce PTP inhibition without the immunosuppressive cellular effects of rapamycin treatment.^{24–26} We acknowledge that applications of this approach will be limited by several factors: the substantial amount of cellular engineering that would be required to generate cell-based CID-inducible systems (expression of both dimerizable SHP1/SHP2 and dimerizable N-SH2 constructs); the potential for addition of dimerization domains to affect the localization and/or binding capacity of a target PTP; and the possibility that exogenously expressed FRB-NSH2 may compete with endogenous SHP2 for binding to other phosphotyrosine-containing proteins. Nevertheless, we suspect that CID-inducible inhibition may serve as an attractive complementary strategy for targeting SHP2 and SHP1 in cellular studies, particularly for GOF SHP2 constructs that prove unresponsive to allosteric SHP2 inhibitors. In addition to cancer-associated GOF SHP2 mutants such as E76K, GOF SHP2 mutants occur in at least 50% of the cases of the developmental disorder Noonan syndrome,^{43,44} and, in principle, CID-induced proximity with N-SH2 could be an effective inhibition strategy for any dimerizable GOF SHP2 mutant that contains a dysfunctional N-SH2 domain.

METHODS

General and Materials. “% PTP Activity” is defined as the initial velocity of a PTP reaction under experimental conditions divided by the initial velocity of a vehicle-only and/or buffer-only control, which is defined as 100% activity. Each data point is an average \pm the standard deviation of at least three independent measurements. The following compounds were purchased commercially and used without further purification: rapamycin (Alfa Aesar), SHP099 (Fisher Scientific), *p*NPP (Fisher Scientific), DiFMUP (Fisher Scientific), pIRS-1 (Biomatik), and DADEpYLIPQQG (Biomatik). Rapamycin, SHP099, DiFMUP, and pIRS-1 were dissolved in DMSO, which served as the vehicle control for all experiments that utilized these compounds. *p*NPP and DADEpYLIPQQG were dissolved in water.

PTP-Encoding Plasmid Vectors. The pET vectors encoding His₆-tagged human SHP2 (pAC005; UniProtKB Q06124, aa 1-541),¹³ human SHP2 CD (pDK012; UniProtKB

Q06124, aa 224-539),²⁹ and human SHP1 CD (pACB149; UniProtKB P29350, aa 243-541)⁴⁵ have been previously described. The vector for the expression of E76K SHP2 was derived from pAC005 using a QuikChange site-directed mutagenesis kit (Agilent) according to the manufacturer's instructions. The pET plasmids for the expression of the C-terminally His₆-tagged CD of FRB-NSH2 [pSJB002; residues 3-103 of SHP2 fused to FRB with an S(GGGGS)₃ linker; Figure S1A], FKBP-SHP2CD [pSJB001; residues 224-539 of SHP2 fused to FKBP12 with an S(GGGGS)₃ linker; Figure S1B], FKBP-(E76K)SHP2 [pBAP024; residues 1-541 of E76K SHP2 fused to FKBP12 with an S(GGGGS)₃ linker; Figure S4], and FKBP-SHP1CD (pBAP021; residues 243-541 of human SHP1 fused to FKBP12 with an S(GGGGS)₃ linker; Figure S6] were purchased from VectorBuilder. The plasmid encoding isolated SHP2 N-SH2 (pET21-NSH2) was a generous gift from Professor Zhong-Yin Zhang (Department of Medicinal Chemistry and Molecular Pharmacology, Purdue University).³³

Protein Expression and Purification. All proteins were expressed and purified using the HisPur Ni-NTA resin (Thermo Scientific) as per the manufacturer's instructions as previously described.⁴⁵ After purification, the proteins were added to a storage buffer (50 mM 3,3-dimethylglutarate at pH 7.0, 1 mM EDTA, and 1 mM TCEP), concentrated, flash-frozen in liquid nitrogen, and stored at -80 °C. Bradford protein assays and a NanoDrop spectrophotometer were used to measure the enzyme concentrations, and SDS-PAGE was used to assess the purity of the protein stocks (Figure S9).

Quenched Phosphatase Activity Assay Using *p*NPP. Quenched PTP assays using *p*NPP as a substrate were carried out in a total volume of 200 μ L, containing the PTP buffer (50 mM 3,3-dimethylglutarate at pH 7.0, 1 mM EDTA, 50 mM sodium chloride), enzyme (varying concentrations, see the figures), and *p*NPP (varying concentrations, see the figures) at 22 °C. PTP reactions were quenched by the addition of 40 μ L of 5 M sodium hydroxide, and the absorbances (405 nm) of 200 μ L of the resulting solutions were measured and adjusted for background absorbance values of pre-quenched controls. To ensure accurate estimation of initial velocities, all reactions were quenched when $\geq 90\%$ of the substrate remained unhydrolyzed. Kinetic constants were determined by fitting the data to the Michaelis–Menten equations using SigmaPlot 12.3.

Continuous Phosphatase Activity Assay with DiFMUP. Continuous PTP assays using DiFMUP as the substrate were carried out in a total volume of 200 μ L containing the PTP buffer, enzyme, N-SH2, FRB-NSH2, and/or rapamycin (varying concentrations, see the figures). After pre-incubations of the proteins and rapamycin (or the DMSO vehicle) for at least 15 min, PTP reactions were started by the addition of DiFMUP (varying concentrations, see the figures). Immediately following DiFMUP addition, the fluorescence of the resulting solutions (excitation: 360 nm; emission: 440 nm) was measured continuously for 1 min, and the slopes of the lines derived from the treated enzyme were compared to the corresponding controls. All slope determinations were derived from linear fits with *R*-squared values of ≥ 0.95 .

Continuous Phosphatase Activity Assays with the Phosphopeptide Substrate. PTP kinetic assays with the phosphopeptide DADEpYLIPQQG were carried out by measuring the increasing absorbance at 282 nm, essentially as described.⁴⁶ Assays were performed at 22 °C in a total

reaction volume of 180 μL of the PTP buffer (see above) in the absence or presence of rapamycin (varying concentrations, see the figures), in the absence or presence of FRB-NSH2 (varying concentrations, see the figures), and in the presence of the appropriate FKBP-fused PTP (50 nM). The reactions were started by the addition of a phosphopeptide (100 μM).

Reversibility Assay. 4 μM FKBP-SHP2CD was incubated for 15 min with 4 μM FRB-NSH2 or a vehicle (storage buffer; see above) in the presence of 7.2 μM rapamycin or a vehicle only in a total volume of 250 μL . 10 μL of the resulting incubation mixture was diluted eightfold, and the PTP activity was measured using the DiFMUP protocol (see above). The His₆-tagged proteins in the remaining incubation mixture were bound to the pre-washed HisPur Ni-NTA resin, washed four times, and eluted. The concentration of the protein was assessed using a NanoDrop spectrophotometer, and the PTP activities of the washed proteins were measured using the DiFMUP protocol (see above).

■ ASSOCIATED CONTENT

SI Supporting Information

The Supporting Information is available free of charge at <https://pubs.acs.org/doi/10.1021/acsomega.2c00780>.

Primary sequences of dimerizable protein constructs; inhibition of SHP2 CD and SHP1 CD by N-SH2; irreversibility of dimerization-induced SHP2 inhibition; Michaelis–Menten kinetic analysis of FKBP-(E76K)SHP2 and FKBP-SHP1CD; and SDS-PAGE analysis of purified proteins (PDF)

■ AUTHOR INFORMATION

Corresponding Author

Anthony C. Bishop – Department of Chemistry, Amherst College, Amherst, Massachusetts 01002, United States;
orcid.org/0000-0001-8394-280X; Email: acbishop@amherst.edu

Authors

Sara J. S. Buck – Department of Chemistry, Amherst College, Amherst, Massachusetts 01002, United States

Bailey A. Plaman – Department of Chemistry, Amherst College, Amherst, Massachusetts 01002, United States;
Present Address: Harvard University, Department of Chemistry and Chemical Biology, Cambridge, MA, 02138, United States

Complete contact information is available at:
<https://pubs.acs.org/doi/10.1021/acsomega.2c00780>

Author Contributions

S.J.S.B. and B.A.P. contributed equally. The experiments were performed by S.J.S.B. and B.A.P. and conceived by A.C.B. in collaboration with S.J.S.B. and B.A.P. The manuscript was written by A.C.B. and B.A.P., and all authors have given approval to the final version of the manuscript.

Funding

Research reported in this publication was supported by the National Institute of General Medical Sciences of the National Institutes of Health under award number R15GM071388 to A.C.B.

Notes

The authors declare no competing financial interest.

■ ACKNOWLEDGMENTS

The authors thank Samuel Korntner for generating the plasmid for the expression of E76K SHP2 and Professor Zhong-Yin Zhang (Purdue University) for generously providing a plasmid that encodes for the isolated N-SH2 domain.

■ REFERENCES

- (1) Tonks, N. K. Protein tyrosine phosphatases: from genes, to function, to disease. *Nat. Rev. Mol. Cell Biol.* **2006**, *7*, 833–846.
- (2) Julien, S. G.; Dubé, N.; Hardy, S.; Tremblay, M. L. Inside the human cancer tyrosine phosphatome. *Nat. Rev. Cancer* **2011**, *11*, 35–49.
- (3) Jiang, Z.-X.; Zhang, Z.-Y. Targeting PTPs with small molecule inhibitors in cancer treatment. *Cancer Metastasis Rev.* **2008**, *27*, 263–272.
- (4) Zhang, S.; Zhang, Z. PTP1B as a drug target: recent developments in PTP1B inhibitor discovery. *Drug Discovery Today* **2007**, *12*, 373–381.
- (5) Easty, D.; Gallagher, W.; Bennett, D. Protein tyrosine phosphatases, new targets for cancer therapy. *Curr. Cancer Drug Targets* **2006**, *6*, 519–532.
- (6) Bialy, L.; Waldmann, H. Inhibitors of protein tyrosine phosphatases: next-generation drugs? *Angew. Chem., Int. Ed.* **2005**, *44*, 3814–3839.
- (7) Blaskovich, M. Drug discovery and protein tyrosine phosphatases. *Curr. Med. Chem.* **2009**, *16*, 2095–2176.
- (8) Zhang, Z.-Y. Drugging the undruggable: Therapeutic potential of targeting protein tyrosine phosphatases. *Acc. Chem. Res.* **2017**, *50*, 122–129.
- (9) Tsutsumi, R.; Ran, H.; Neel, B. G.; Neel, B. G. Off-target inhibition by active site-targeting SHP 2 inhibitors. *FEBS Open Bio* **2018**, *8*, 1405–1411.
- (10) Chen, Y.-N. P.; LaMarche, M. J.; Chan, H. M.; Fekkes, P.; Garcia-Fortanet, J.; Acker, M. G.; Antonakos, B.; Chen, C. H.-T.; Chen, Z.; Cooke, V. G.; Dobson, J. R.; Deng, Z.; Fei, F.; Firestone, B.; Fodor, M.; Fridrich, C.; Gao, H.; Grunenfelder, D.; Hao, H.-X.; Jacob, J.; Ho, S.; Hsiao, K.; Kang, Z. B.; Karki, R.; Kato, M.; Larrow, J.; La Bonte, L. R.; Lenoir, F.; Liu, G.; Liu, S.; Majumdar, D.; Meyer, M. J.; Palermo, M.; Perez, L.; Pu, M.; Price, E.; Quinn, C.; Shakya, S.; Shultz, M. D.; Slisz, J.; Venkatesan, K.; Wang, P.; Warmuth, M.; Williams, S.; Yang, G.; Yuan, J.; Zhang, J.-H.; Zhu, P.; Ramsey, T.; Keen, N. J.; Sellers, W. R.; Stams, T.; Fortin, P. D. Allosteric inhibition of SHP2 phosphatase inhibits cancers driven by receptor tyrosine kinases. *Nature* **2016**, *535*, 148–152.
- (11) Perron, M. D.; Chowdhury, S.; Aubry, I.; Purisima, E.; Tremblay, M. L.; Saragovi, H. U. Allosteric noncompetitive small molecule selective inhibitors of CD45 tyrosine phosphatase suppress T-cell receptor signals and inflammation in vivo. *Mol. Pharmacol.* **2014**, *85*, 553–563.
- (12) Krishnan, N.; Koveal, D.; Miller, D. H.; Xue, B.; Akshinthala, S. D.; Kragelj, J.; Jensen, M. R.; Gauss, C.-M.; Page, R.; Blackledge, M.; Muthuswamy, S. K.; Peti, W.; Tonks, N. K. Targeting the disordered C terminus of PTP1B with an allosteric inhibitor. *Nat. Chem. Biol.* **2014**, *10*, 558–566.
- (13) Marsh-Armstrong, B.; Fajnzylber, J. M.; Korntner, S.; Plaman, B. A.; Bishop, A. C. The allosteric site on SHP2's protein tyrosine phosphatase domain is targetable with druglike small molecules. *ACS Omega* **2018**, *3*, 15763–15770.
- (14) Fodor, M.; Price, E.; Wang, P.; Lu, H.; Argintaru, A.; Chen, Z.; Glick, M.; Hao, H.-X.; Kato, M.; Koenig, R.; LaRochelle, J. R.; Liu, G.; McNeill, E.; Majumdar, D.; Nishiguchi, G. A.; Perez, L. B.; Paris, G.; Quinn, C. M.; Ramsey, T.; Sendzik, M.; Shultz, M. D.; Williams, S. L.; Stams, T.; Blacklow, S. C.; Acker, M. G.; LaMarche, M. J. Dual allosteric inhibition of SHP2 phosphatase. *ACS Chem. Biol.* **2018**, *13*, 647–656.
- (15) Hansen, S. K.; Cancelli, M. T.; Shiau, T. P.; Kung, J.; Chen, T.; Erlanson, D. A. Allosteric inhibition of PTP1B activity by selective

modification of a non-active site cysteine residue. *Biochemistry* **2005**, *44*, 7704–7712.

(16) Wiesmann, C.; Barr, K. J.; Kung, J.; Zhu, J.; Erlanson, D. A.; Shen, W.; Fahr, B. J.; Zhong, M.; Taylor, L.; Randal, M.; McDowell, R. S.; Hansen, S. K. Allosteric inhibition of protein tyrosine phosphatase 1B. *Nat. Struct. Mol. Biol.* **2004**, *11*, 730–737.

(17) LaRochelle, J. R.; Fodor, M.; Vemulapalli, V.; Mohseni, M.; Wang, P.; Stams, T.; LaMarche, M. J.; Chopra, R.; Acker, M. G.; Blacklow, S. C. Structural reorganization of SHP2 by oncogenic mutations and implications for oncoprotein resistance to allosteric inhibition. *Nat. Commun.* **2018**, *9*, 4508.

(18) Pádua, R. A. P.; Sun, Y.; Marko, I.; Pitsawong, W.; Stiller, J. B.; Otten, R.; Kern, D. Mechanism of activating mutations and allosteric drug inhibition of the phosphatase SHP2. *Nat. Commun.* **2018**, *9*, 4507.

(19) Sun, X.; Ren, Y.; Gunawan, S.; Teng, P.; Chen, Z.; Lawrence, H.; Cai, J.; Lawrence, N.; Wu, J. Selective inhibition of leukemia-associated SHP2E69K mutant by the allosteric SHP2 inhibitor SHP099. *Leukemia* **2018**, *32*, 1246–1249.

(20) Hoffman, H. E.; Blair, E. R.; Johndrow, J. E.; Bishop, A. C. Allele-specific inhibitors of protein tyrosine phosphatases. *J. Am. Chem. Soc.* **2005**, *127*, 2824–2825.

(21) Zhang, X.-Y.; Bishop, A. C. Site-specific incorporation of allosteric-inhibition sites in a protein tyrosine phosphatase. *J. Am. Chem. Soc.* **2007**, *129*, 3812–3813.

(22) Chio, C. M.; Yu, X.; Bishop, A. C. Rational design of allosteric-inhibition sites in classical protein tyrosine phosphatases. *Bioorg. Med. Chem.* **2015**, *23*, 2828–2838.

(23) Plaman, B. A.; Chan, W. C.; Bishop, A. C. Chemical activation of divergent protein tyrosine phosphatase domains with cyanine-based bisarsenicals. *Sci. Rep.* **2019**, *9*, 16148.

(24) Voß, S.; Klewer, L.; Wu, Y.-W. Chemically induced dimerization: reversible and spatiotemporal control of protein function in cells. *Curr. Opin. Chem. Biol.* **2015**, *28*, 194–201.

(25) Putyrski, M.; Schultz, C. Protein translocation as a tool: The current rapamycin story. *FEBS Lett.* **2012**, *586*, 2097–2105.

(26) Fegan, A.; White, B.; Carlson, J. C. T.; Wagner, C. R. Chemically controlled protein assembly: Techniques and applications. *Chem. Rev.* **2010**, *110*, 3315–3336.

(27) Chen, J.; Zheng, X. F.; Brown, E. J.; Schreiber, S. L. Identification of an 11-kDa FKBP12-rapamycin-binding domain within the 289-kDa FKBP12-rapamycin-associated protein and characterization of a critical serine residue. *Proc. Natl. Acad. Sci. U.S.A.* **1995**, *92*, 4947–4951.

(28) Camacho-Soto, K.; Castillo-Montoya, J.; Tye, B.; Ogunleye, L. O.; Ghosh, I. Small molecule gated split-tyrosine phosphatases and orthogonal split-tyrosine kinases. *J. Am. Chem. Soc.* **2014**, *136*, 17078–17086.

(29) Yuan, X.; Bu, H.; Zhou, J.; Yang, C.-Y.; Zhang, H. Recent advances of SHP2 inhibitors in cancer therapy: Current development and clinical application. *J. Med. Chem.* **2020**, *63*, 11368–11396.

(30) Shen, D.; Chen, W.; Zhu, J.; Wu, G.; Shen, R.; Xi, M.; Sun, H. Therapeutic potential of targeting SHP2 in human developmental disorders and cancers. *Eur. J. Med. Chem.* **2020**, *190*, 112117.

(31) Neel, B. G.; Gu, H.; Pao, L. The 'Shp'ing news: SH2 domain-containing tyrosine phosphatases in cell signaling. *Trends Biochem. Sci.* **2003**, *28*, 284–293.

(32) Hof, P.; Pluskey, S.; Dhe-Paganon, S.; Eck, M. J.; Shoelson, S. E. Crystal structure of the tyrosine phosphatase SHP-2. *Cell* **1998**, *92*, 441–450.

(33) Yu, Z.-H.; Xu, J.; Walls, C. D.; Chen, L.; Zhang, S.; Zhang, R.; Wu, L.; Wang, L.; Liu, S.; Zhang, Z.-Y. Structural and mechanistic insights into LEOPARD syndrome-associated SHP2 mutations. *J. Biol. Chem.* **2013**, *288*, 10472–10482.

(34) Banaszynski, L. A.; Liu, C. W.; Wandless, T. J. Characterization of the FKBP-Rapamycin-FRB Ternary Complex. *J. Am. Chem. Soc.* **2005**, *127*, 4715–4721.

(35) Sarmiento, M.; Puius, Y. A.; Vetter, S. W.; Keng, Y.-F.; Wu, L.; Zhao, Y.; Lawrence, D. S.; Almo, S. C.; Zhang, Z.-Y. Structural Basis

of Plasticity in Protein Tyrosine Phosphatase 1B Substrate Recognition. *Biochemistry* **2000**, *39*, 8171–8179.

(36) Lee, C.-H.; Kominos, D.; Jacques, S.; Margolis, B.; Schlessinger, J.; Shoelson, S. E.; Kuriyan, J. Crystal structures of peptide complexes of the amino-terminal SH2 domain of the Syp tyrosine phosphatase. *Structure* **1994**, *2*, 423–438.

(37) Tartaglia, M.; Gelb, B. D. Germ-line and somatic PTPN11 mutations in human disease. *Eur. J. Med. Genet.* **2005**, *48*, 81–96.

(38) Mohi, M. G.; Neel, B. G. The role of Shp2 (PTPN11) in cancer. *Curr. Opin. Genet. Dev.* **2007**, *17*, 23–30.

(39) Pandey, R.; Saxena, M.; Kapur, R. Role of SHP2 in hematopoiesis and leukemogenesis. *Curr. Opin. Hematol.* **2017**, *24*, 307–313.

(40) Yu, W.-M.; Daino, H.; Chen, J.; Bunting, K. D.; Qu, C.-K. Effects of a leukemia-associated gain-of-function mutation of SHP-2 phosphatase on interleukin-3 signaling. *J. Biol. Chem.* **2006**, *281*, 5426–5434.

(41) Andersen, J. N.; Mortensen, O. H.; Peters, G. H.; Drake, P. G.; Iversen, L. F.; Olsen, O. H.; Jansen, P. G.; Andersen, H. S.; Tonks, N. K.; Møller, N. P. H. Structural and evolutionary relationships among protein tyrosine phosphatase domains. *Mol. Cell. Biol.* **2001**, *21*, 7117–7136.

(42) O'Reilly, A. M.; Neel, B. G. Structural determinants of SHP-2 function and specificity in *Xenopus* mesoderm induction. *Mol. Cell. Biol.* **1998**, *18*, 161–177.

(43) Bentires-Alj, M.; Paez, J. G.; David, F. S.; Keilhack, H.; Halmos, B.; Naoki, K.; Maris, J. M.; Richardson, A.; Bardelli, A.; Sugarbaker, D. J.; Richards, W. G.; Du, J.; Girard, L.; Minna, J. D.; Loh, M. L.; Fisher, D. E.; Velculescu, V. E.; Vogelstein, B.; Meyerson, M.; Sellers, W. R.; Neel, B. G. Activating mutations of the Noonan syndrome-associated SHP2/PTPN11 gene in human solid tumors and adult acute myelogenous leukemia. *Cancer Res.* **2004**, *64*, 8816–8820.

(44) Tartaglia, M.; Gelb, B. D. Noonan syndrome and related disorders: Genetics and pathogenesis. *Annu. Rev. Genomics Hum. Genet.* **2005**, *6*, 45–68.

(45) Chio, C. M.; Lim, C. S.; Bishop, A. C. Targeting a cryptic allosteric site for selective inhibition of the oncogenic protein tyrosine phosphatase Shp2. *Biochemistry* **2015**, *54*, 497–504.

(46) Zhang, Z. Y.; Maclean, D.; Thiemesfleter, A. M.; Roeske, R. W.; Dixon, J. E. A Continuous Spectrophotometric and Fluorometric Assay for Protein Tyrosine Phosphatase Using Phosphotyrosine-Containing Peptides. *Anal. Biochem.* **1993**, *211*, 7–15.